WJPMR, 2026, 12(4), 406-414

Research Article

WORLD JOURNAL OF PHARMACEUTICAL AND MEDICAL RESEARCH

www.wjpmr.com

Impact Factor: 7.555

ISSN (O): 2455-3301

ISSN (P): 3051-2557

Coden USA: WJPMBB

IN SILICO INVESTIGATION OF PHYTOCONSTITUENTS OF MEDICINAL HERB PLUMBAGO ZEYLANICA AGAINST CANCER BY MOLECULAR DOCKING

Dr. Priyanka K. Dighde*

Ph.D. Scholar, Department of Rasashastra, Datta Meghe Institute of Higher Education and Research (Deemed University), Wardha, Maharashtra, India.
Assistant Professor (Rasashastra and Bhaishajyakalpana) Shri Ayurveda Mahavidyalaya, Nagpur, Maharashtra, India.

***Corresponding Author: Dr. Priyanka K. Dighde**

Ph.D. Scholar, Department of Rasashastra, Datta Meghe Institute of Higher Education and Research (Deemed University), Wardha, Maharashtra, India.
Assistant Professor (Rasashastra and Bhaishajyakalpana) Shri Ayurveda Mahavidyalaya, Nagpur, Maharashtra, India. **DOI:** https://doi.org/10.5281/zenodo.19434972

How to cite this Article: Dr. Priyanka K. Dighde*. (2026). In Silico Investigation Of Phytoconstituents Of Medicinal Herb Plumbago Zeylanica Against Cancer By Molecular Docking. World Journal of Pharmaceutical and Medical Research, 12(4), 406–414.

Article Received on 05/03/2026 **Article Revised on 25/03/2026** **Article Published on 04/04/2026**

ABSTRACT

Background: Plumbago zeylanica Linn. (Chitrak) is a traditional medicinal herb in the Ayurvedic pharmacopoeia, valued for its anticancer, anti-inflammatory, and antimicrobial properties. While plumbagin, the principal bioactive naphthoquinone from this plant, has been extensively investigated, other phytoconstituents including chitranone and droserone remain largely unexplored as potential anticancer candidates. **Objective:** This study aimed to evaluate the anticancer potential of chitranone and droserone, two naphthoquinone derivatives from P. zeylanica, against the epidermal growth factor receptor (EGFR) kinase domain (PDB ID: 8A2B) using molecular docking and ADMET prediction, with doxorubicin as a reference standard. **Methods:** Phytoconstituents were identified from the IMPPAT database. The EGFR kinase domain crystal structure (resolution: 1.69 Å) was validated via Ramachandran plot analysis using PROCHECK. Molecular docking was performed using Auto Dock Vina 1.5.6. Binding interactions were visualized using Discovery Studio and PyRx. ADMET profiling was conducted using Swiss ADME and ProTox-II. **Results:** Chitranone demonstrated the highest binding affinity (−10.5 kcal/mol) with three hydrogen bonds and 16 total interactions, surpassing doxorubicin (−8.8 kcal/mol, four hydrogen bonds, 11 interactions). Droserone showed a binding energy of −7.1 kcal/mol with one hydrogen bond and seven interactions. Both naphthoquinones exhibited zero Lipinski violations, high gastrointestinal absorption, and favorable drug-likeness. Chitranone had a predicted LD_{50} of 1000 mg/kg (toxicity class 4) vs. 205 mg/kg (toxicity class 3) for doxorubicin. **Conclusion:** Chitranone exhibited superior binding affinity to the EGFR kinase domain compared to doxorubicin, suggesting its potential as a lead compound for anticancer drug development. Both naphthoquinones warrant further in vitro and in vivo validation.

KEYWORDS: *Plumbago zeylanica, Chitranone, Droserone, EGFR, Molecular docking, ADMET, Naphthoquinone, Anticancer, In silico.*

1. INTRODUCTION

Cancer remains one of the foremost public health challenges worldwide, accounting for approximately 10 million deaths annually, thereby necessitating an ongoing search for novel therapeutic agents with improved efficacy and reduced adverse effects.[1] The epidermal growth factor receptor (EGFR), a transmembrane receptor tyrosine kinase belonging to the ErbB family, plays a pivotal role in cellular proliferation, differentiation, migration, and survival signaling.[2] Aberrant EGFR activation through mutation or overexpression is implicated in numerous malignancies, particularly non-small-cell lung cancer (NSCLC), colorectal cancer, and head and neck cancers, making it a critical therapeutic target in oncology.[3]

Medicinal plants have historically served as invaluable reservoirs of bioactive compounds for drug discovery, with an estimated 49% of currently used anticancer small molecules being either natural products or their direct derivatives.[4] In this context, Plumbago zeylanica Linn. (commonly known as Chitrak in Ayurveda), a perennial

herbaceous plant belonging to the family Plumbaginaceae distributed across tropical and subtropical regions, has garnered considerable attention for its diverse pharmacological properties.[5,6] This plant has been employed in the Indian Ayurvedic system of medicine for over 2,500 years for treating skin diseases, digestive disorders, rheumatic pain, hemorrhoids, and inflammatory conditions.[7]

The phytochemical profile of P. zeylanica is characterized by naphthoquinones, flavonoids, alkaloids, coumarins, triterpenoids, and glycosides.[8] Among these, plumbagin (5-hydroxy-2-methyl-1,4-naphthoquinone) is the most extensively studied constituent, with well-documented anticancer and antiproliferative activities against breast, lung, prostate, pancreatic, esophageal, and squamous cell carcinomas.[9–11] Plumbagin exerts its anticancer effects through the modulation of multiple signaling cascades, including inhibition of NF-κB, STAT3, PI3K/AKT, and Bcl-2 pathways.[9–12]

However, beyond plumbagin, P. zeylanica harbors several other naphthoquinone derivatives whose anticancer potential remains relatively underexplored. Chitranone, a binaphthoquinone (Molecular weight- 374.34 g/mol; $C_{22}H_{14}O_6$), was first isolated from the roots of P. zeylanica alongside zeylanone, maritinone, and 2-methylnaphthazarin.[13] Droserone (3,5-dihydroxy-2-methyl-1,4-naphthoquinone; Molecular weight- 204.18 g/mol; $C_{11}H_8O_4$) is a naturally occurring naphthoquinone found in the *Plumbaginaceae* and Droseraceae families.[14] Recent investigations have demonstrated droserone's antiviral activity against measles virus and its antiausterity activity against pancreatic cancer cells, suggesting broader pharmacological significance.[15,16]

Molecular docking has emerged as an indispensable computational tool in structure-based drug discovery, enabling rapid prediction of ligand–receptor binding affinities and interaction profiles. The present study employs in silico molecular docking to evaluate the binding interactions of chitranone and droserone with the EGFR kinase domain (PDB ID: 8A2B), complemented by ADMET profiling. Doxorubicin, a widely used anthracycline chemotherapeutic agent, was used as a reference standard.

2. MATERIALS AND METHODS

2.1 Identification of Phytoconstituents

The phytoconstituents of P. zeylanica were traced from the Indian Medicinal Plants, Phytochemistry and Therapeutics (IMPPAT) database.[17] Chitranone and droserone were selected for molecular docking based on their structural characteristics and reported biological activities.

2.2 Protein Target Selection and Preparation

The three-dimensional crystal structure of the EGFR kinase domain (PDB ID: 8A2B), classified as a transferase, was retrieved from the RCSB Protein Data Bank. This structure represents the EGFR kinase domain with L858R/V948R mutations, from Homo sapiens expressed in Spodoptera frugiperda, resolved at 1.69 Å by X-ray crystallography (R-Value Free: 0.258; R-Value Work: 0.210; R-Value Observed: 0.212).[4] Protein preparation involved removing co-crystallized ligands, water molecules, and heteroatoms, adding hydrogen atoms, and performing energy minimization using UCSF Chimera.

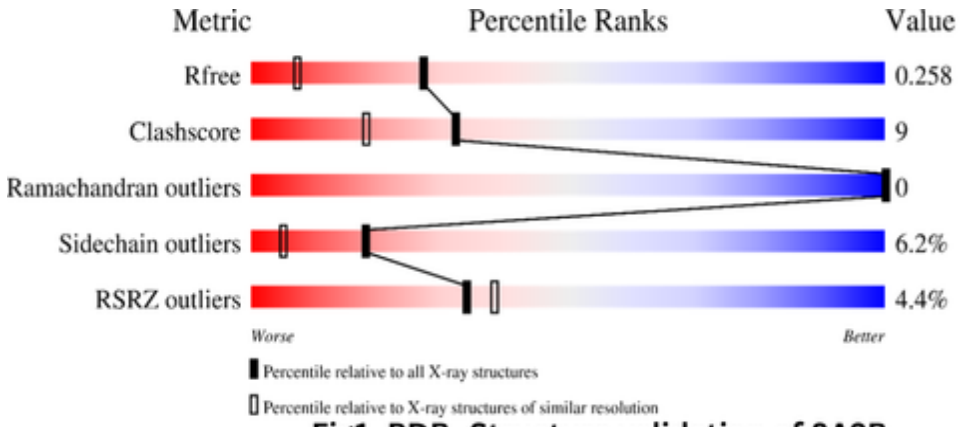

Fig1- PDB- Structure validation of 8A2B

Stereochemical quality was validated via Ramachandran plot analysis using PROCHECK.[18] Of 239 non-glycine, non-proline residues, 223 (93.3%) occupied the most favored regions [A,B,L], 15 (6.3%) were in additionally allowed regions [a,b,l,p], 1 (0.4%) in generously allowed regions, and 0 (0.0%) in disallowed regions. The total number of residues was 272, with 3 end-residues, 15 glycine and 15 proline residues.

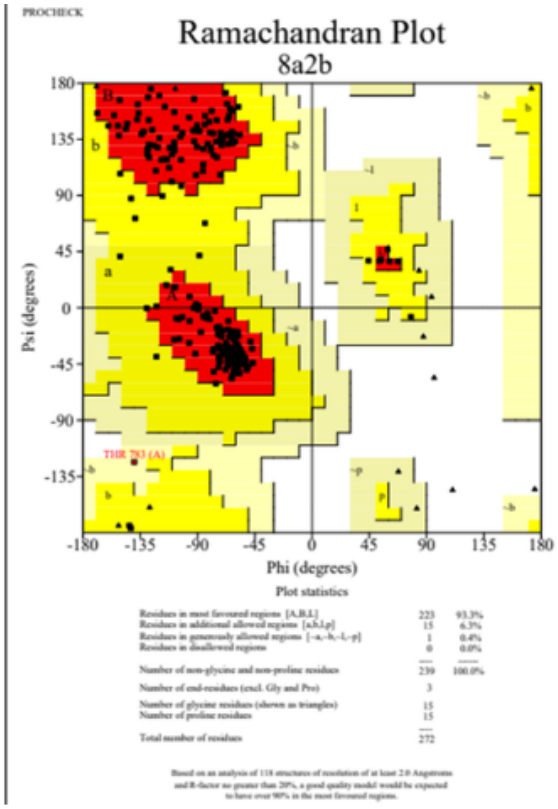

Fig 2 (A)- Ramchandran Plot

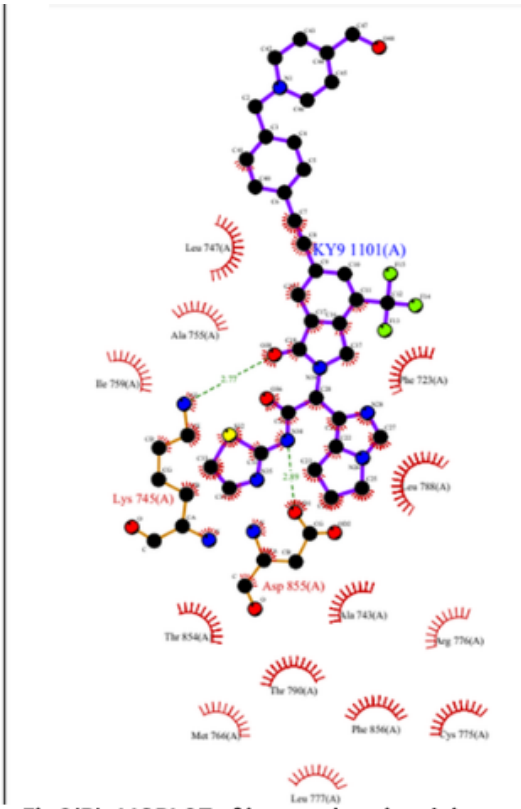

Fig 2(B)- LIGPLOT of interactions involving ligand KY9

2.3 Ligand Preparation

Three-dimensional structures of chitranone (28 atoms, 31 bonds, 1 rotatable bond, TPSA: 108.74 Å², logP: 3.28, molecular refractivity: 100.98), droserone (15 atoms, 16 bonds, 0 rotatable bonds, TPSA: 74.60 Å², logP: 1.45, molecular refractivity: 53.22), and doxorubicin (39 atoms, 43 bonds, 5 rotatable bonds, TPSA: 206.07 Å², logP: 0.7, molecular refractivity: 132.66) were obtained from PubChem. The ligands were prepared by optimizing their geometry, assigning Gasteiger charges, and converting them to PDBQT format for docking using AutoDock Tools.

2.4 Molecular Docking Protocol

Molecular docking studies were performed using Auto Dock Vina version 1.5.6.[19] The grid box was centered on the active site of the EGFR kinase domain with appropriate dimensions to encompass the binding pocket. The exhaustiveness parameter was set to ensure thorough conformational sampling. The docking results were ranked based on binding energy (kcal/mol), and the best poses were selected for interaction analysis. Binding interactions, including hydrogen bonds, hydrophobic contacts, electrostatic interactions, and pi-stacking interactions, were analyzed and visualized using PyRx, Discovery Studio Visualizer molecular graphics software.

2.5 ADMET and Drug-likeness Prediction

Pharmacokinetic and drug-likeness properties of chitranone, droserone, and doxorubicin were predicted using Swiss ADME.[20] Parameters evaluated included physicochemical properties, lipophilicity, water solubility, pharmacokinetics (gastrointestinal absorption, blood-brain barrier permeability, P-glycoprotein substrate status, and cytochrome P450 enzyme inhibition), and drug-likeness criteria (Lipinski, Ghose, Veber, Egan, and Muegge filters). Toxicity was predicted using ProTox-II[21], which provided LD_{50} values, toxicity class, organ toxicity, Tox21 nuclear receptor and stress response pathways, molecular initiating events, and metabolic enzyme interactions.

3. RESULTS

3.1 Protein Structure Validation

The Ramachandran plot analysis confirmed excellent stereochemical quality with 93.3% of residues in most favored regions and none in disallowed regions.[18] The co-crystallized ligand KY9 1101(A) showed interactions with Leu747, Ala755, Ile759, Phe723, Lys745, Leu788, Asp855, Ala743, Arg776, Thr854, Thr790, Met766, Phe856, Lys775, and Leu777, confirming the binding site architecture.

3.2 Molecular Docking Analysis

The docking results revealed differential binding affinities summarized in Table 1.

Table 1: Molecular docking results of ligands with EGFR kinase domain (PDB ID: 8A2B).

Ligand	Binding Energy (kcal/mol)	H-bonds	Total Interactions	Key Interacting Residues
Chitranone	−10.5	3	16	ARG858, ASP855, LEU788, MET766, PHE723, ILE759, LEU747, LEU777
Droserone	−7.1	1	7	ASP855, ARG858, LEU788, MET766, LEU777
Doxorubicin	−8.8	4	11	MET793, THR854, ASP855, VAL726, LEU718, ARG841, LEU844, ALA743

3.2.1 Chitranone–EGFR Interactions

Chitranone demonstrated the highest binding affinity (−10.5 kcal/mol) with 16 total interactions. Three conventional hydrogen bonds were identified: ARG858 as H-donor to ligand H-acceptor (2.90 Å; angle XDA: 64.27°, DAY: 97.17°), ligand H-donor to ligand H-acceptor (2.25 Å; angle DHA: 114.86°), and ligand H-donor to ASP H-acceptor (2.42 Å; angle DHA: 124.92°). Two pi-cation electrostatic interactions were observed with ARG858 (4.26 and 4.79 Å). A pi-sigma hydrophobic interaction was formed with LEU788 (3.49 Å), and a pi-pi T-shaped interaction with PHE723 (5.12 Å). Nine pi-alkyl contacts engaged MET766 (two contacts), LEU777, LEU747 (two contacts), ILE759, and ARG858 (two contacts), with distances ranging from 4.41 to 5.41 Å.

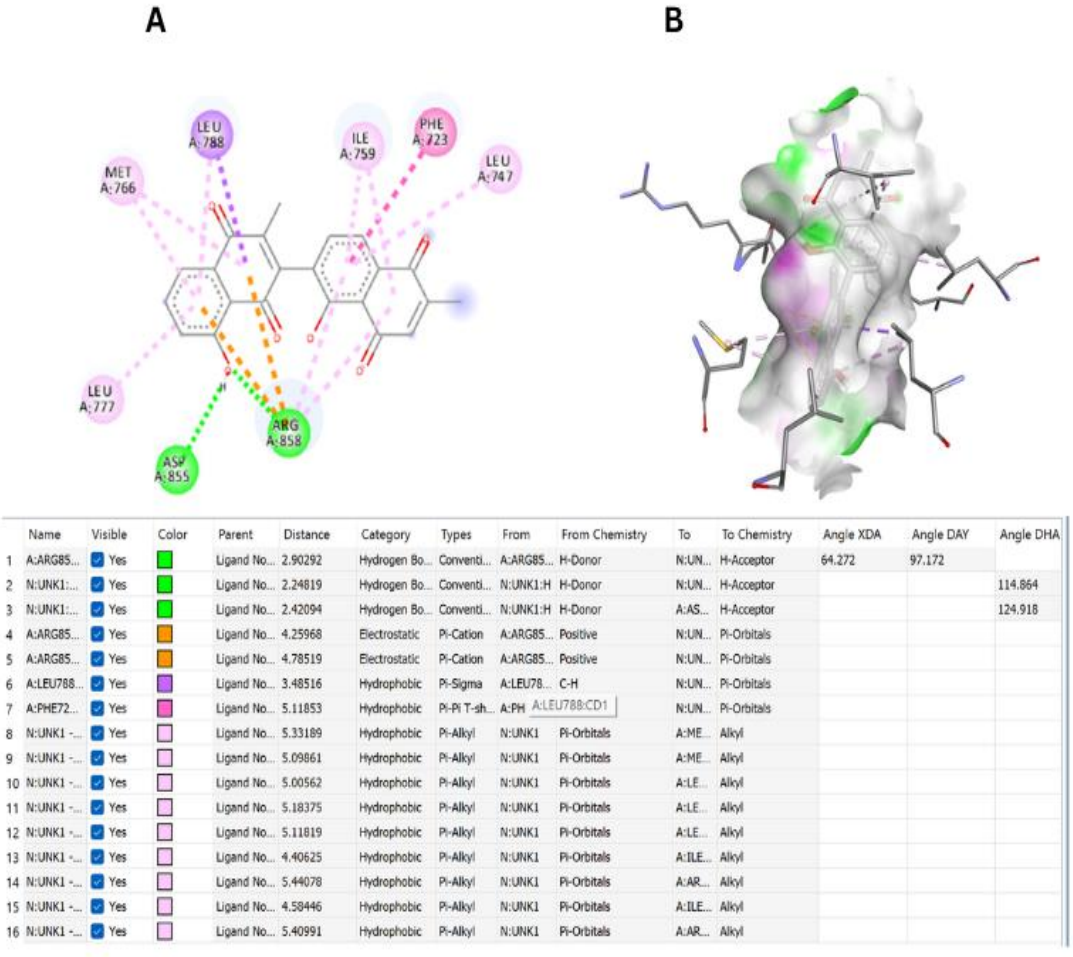

	Name	Visible	Color	Parent	Distance	Category	Types	From	From Chemistry	To	To Chemistry	Angle XDA	Angle DAY	Angle DHA
1	A:ARG85...	Yes		Ligand No...	2.90292	Hydrogen Bo...	Conventi...	A:ARG85...	H-Donor	N:UN...	H-Acceptor	64.272	97.172	
2	N:UNK1:...	Yes		Ligand No...	2.24819	Hydrogen Bo...	Conventi...	N:UNK1:H	H-Donor	N:UN...	H-Acceptor			114.864
3	N:UNK1:...	Yes		Ligand No...	2.42094	Hydrogen Bo...	Conventi...	N:UNK1:H	H-Donor	A:AS...	H-Acceptor			124.918
4	A:ARG85...	Yes		Ligand No...	4.25968	Electrostatic	Pi-Cation	A:ARG85...	Positive	N:UN...	Pi-Orbitals			
5	A:ARG85...	Yes		Ligand No...	4.78519	Electrostatic	Pi-Cation	A:ARG85...	Positive	N:UN...	Pi-Orbitals			
6	A:LEU788...	Yes		Ligand No...	3.48516	Hydrophobic	Pi-Sigma	A:LEU78...	C-H	N:UN...	Pi-Orbitals			
7	A:PHE72...	Yes		Ligand No...	5.11853	Hydrophobic	Pi-Pi T-sh...	A:PH	A:LEU788:CD1	N:UN...	Pi-Orbitals			
8	N:UNK1 -...	Yes		Ligand No...	5.33189	Hydrophobic	Pi-Alkyl	N:UNK1	Pi-Orbitals	A:ME...	Alkyl			
9	N:UNK1 -...	Yes		Ligand No...	5.09861	Hydrophobic	Pi-Alkyl	N:UNK1	Pi-Orbitals	A:ME...	Alkyl			
10	N:UNK1 -...	Yes		Ligand No...	5.00562	Hydrophobic	Pi-Alkyl	N:UNK1	Pi-Orbitals	A:LE...	Alkyl			
11	N:UNK1 -...	Yes		Ligand No...	5.18375	Hydrophobic	Pi-Alkyl	N:UNK1	Pi-Orbitals	A:LE...	Alkyl			
12	N:UNK1 -...	Yes		Ligand No...	5.11819	Hydrophobic	Pi-Alkyl	N:UNK1	Pi-Orbitals	A:LE...	Alkyl			
13	N:UNK1 -...	Yes		Ligand No...	4.40625	Hydrophobic	Pi-Alkyl	N:UNK1	Pi-Orbitals	A:ILE...	Alkyl			
14	N:UNK1 -...	Yes		Ligand No...	5.44078	Hydrophobic	Pi-Alkyl	N:UNK1	Pi-Orbitals	A:AR...	Alkyl			
15	N:UNK1 -...	Yes		Ligand No...	4.58446	Hydrophobic	Pi-Alkyl	N:UNK1	Pi-Orbitals	A:ILE...	Alkyl			
16	N:UNK1 -...	Yes		Ligand No...	5.40991	Hydrophobic	Pi-Alkyl	N:UNK1	Pi-Orbitals	A:AR...	Alkyl			

Fig-3- Chitranone- EGFR interactions -(A)– 2D representation and (B) binding mode representation

3.2.2 Droserone–EGFR Interactions

Droserone showed a binding energy of −7.1 kcal/mol with seven interactions. One conventional hydrogen bond was formed between a ligand H-donor and ASP H-acceptor (2.56 Å; angle DHA: 101.62°, HAY: 99.82°). Two pi-cation electrostatic interactions involved ARG858 (4.06 and 4.76 Å). A pi-sigma interaction with LEU788 (3.54 Å) and three pi-alkyl contacts with MET766 (5.22 Å) and LEU777 (4.99 and 4.84 Å) completed the profile.

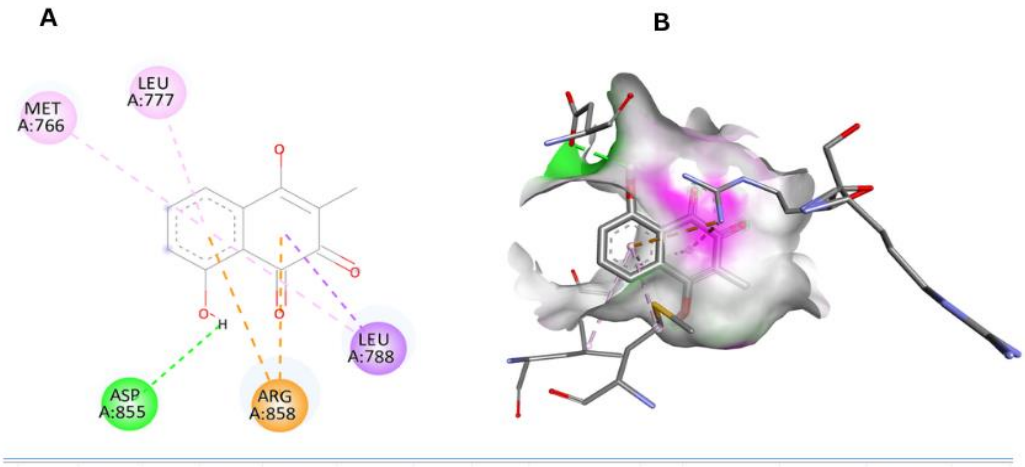

	Name	Visible	Color	Parent	Distance	Category	Types	From	From Chemistry	To	To Chemistry	Angle DHA	Angle HAY	Theta
1	N:UNK1:...	Yes		Ligand No...	2.55735	Hydrogen Bo...	Conventi...	N:UNK1:H	H-Donor	A:AS...	H-Acceptor	101.623	99.821	
2	A:ARG85...	Yes		Ligand No...	4.06076	Electrostatic	Pi-Cation	A:ARG85...	Positive	N:UN...	Pi-Orbitals			14.815
3	A:ARG85...	Yes		Ligand No...	4.76307	Electrostatic	Pi-Cation	A:ARG85...	Positive	N:UN...	Pi-Orbitals			34.574
4	A:LEU788...	Yes		Ligand No...	3.54292	Hydrophobic	Pi-Sigma	A:LEU78...	C-H	N:UN...	Pi-Orbitals			5.556
5	N:UNK1 -...	Yes		Ligand No...	5.21997	Hydrophobic	Pi-Alkyl	N:UNK1	Pi-Orbitals	A:ME...	Alkyl			
6	N:UNK1 -...	Yes		Ligand No...	4.99176	Hydrophobic	Pi-Alkyl	N:UNK1	Pi-Orbitals	A:LE...	Alkyl			
7	N:UNK1 -...	Yes		Ligand No...	4.8381	Hydrophobic	Pi-Alkyl	N:UNK1	Pi-Orbitals	A:LE...	Alkyl			

Fig 4- Droserone–EGFR Interactions- (A)- 2D representation and (B) -binding mode representation

3.2.3 Doxorubicin–EGFR Interactions

Doxorubicin showed a binding energy of −8.8 kcal/mol with 11 interactions. Four hydrogen bonds involved MET793 (3.39 Å), THR854 (2.79 Å), and two ligand–ASP/ligand contacts (2.25 and 2.20 Å). Two pi-sigma interactions with LEU718 (3.64 Å) and VAL726 (3.89 Å), two alkyl contacts with ARG841 and LEU844, and three pi-alkyl contacts with ALA743, LEU844, and LEU completed the interaction profile.

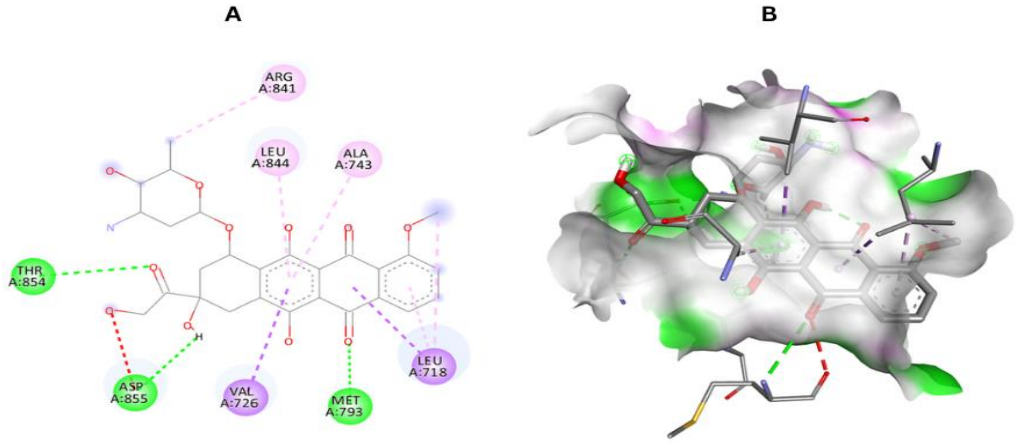

	Name	Visible	Color	Parent	Distance	Category	Types	From	From Chemistry	To	To Chemistry	Angle XDA	Angle DAY	Angle
1	A:MET79...	Yes		Ligand No...	3.38537	Hydrogen Bo...	Conventi...	A:MET79...	H-Donor	N:UN...	H-Acceptor	30.242	175.091	
2	A:THR85...	Yes		Ligand No...	2.78648	Hydrogen Bo...	Conventi...	A:THR85...	H-Donor	N:UN...	H-Acceptor	84.976	136.007	
3	N:UNK1:...	Yes		Ligand No...	2.24658	Hydrogen Bo...	Conventi...	N:UNK1:H	H-Donor	A:AS...	H-Acceptor			158.081
4	N:UNK1:...	Yes		Ligand No...	2.20279	Hydrogen Bo...	Conventi...	N:UNK1:H	H-Donor	N:UN...	H-Acceptor			96.475
5	A:LEU718...	Yes		Ligand No...	3.63588	Hydrophobic	Pi-Sigma	A:LEU71...	C H-Donor	N:UN...	Pi-Orbitals			
6	A:VAL726...	Yes		Ligand No...	3.8892	Hydrophobic	Pi-Sigma	A:VAL72...	C-H	N:UN...	Pi-Orbitals			
7	N:UNK1:...	Yes		Ligand No...	4.24178	Hydrophobic	Alkyl	N:UNK1:C	Alkyl	A:AR...	Alkyl			
8	N:UNK1:...	Yes		Ligand No...	4.22283	Hydrophobic	Alkyl	N:UNK1:C	Alkyl	A:LE...	Alkyl			
9	N:UNK1 -...	Yes		Ligand No...	4.5978	Hydrophobic	Pi-Alkyl	N:UNK1	Pi-Orbitals	A:AL...	Alkyl			
10	N:UNK1 -...	Yes		Ligand No...	5.34985	Hydrophobic	Pi-Alkyl	N:UNK1	Pi-Orbitals	A:LE...	Alkyl			
11	N:UNK1 -...	Yes		Ligand No...	4.13755	Hydrophobic	Pi-Alkyl	N:UNK1	Pi-Orbitals	A:LE...	Alkyl			

Fig 5- Doxorubicin–EGFR Interactions- (A)- 2D representation and (B) -binding mode representation

3.3 ADMET and Drug-likeness Profiling

The Swiss ADME profiles are summarized in Table 2.

Table 2: Comparative physicochemical, pharmacokinetic, and drug-likeness profiles (Swiss ADME).

Parameter	Chitranone	Droserone	Doxorubicin
Formula	$C_{22}H_{14}O_6$	$C_{11}H_8O_4$	$C_{27}H_{29}NO_{11}$
Molecular Weight (g/mol)	374.34	204.18	543.52
Rotatable Bonds	1	0	5
H-bond Acceptors / Donors	6 / 2	4 / 2	12 / 6
TPSA (Å²)	108.74	74.60	206.07
Consensus Log P	2.88	1.13	0.52
GI Absorption	High	High	Low
BBB Permeant	No	No	No
P-gp Substrate	No	No	Yes
CYP1A2 / CYP2C9 / CYP3A4 Inh.	Yes / Yes / Yes	Yes / No / Yes	No / No / No
CYP2C19 / CYP2D6 Inh.	No / No	No / No	No / No
Lipinski	Yes; 0 violation	Yes; 0 violation	No; 3 violations
Bioavailability Score	0.55	0.85	0.17
PAINS	2: ene_one_D, quinone_A	2: imine_one_A, quinone_D	1: quinone_A
Brenk	0 alert	1: diketo_group	1: hydroquinone
Leadlikeness	No; MW>350, XLOGP3>3.5	No; MW<250	No; MW>350
Synthetic Accessibility	3.52	2.62	5.81

3.4 Toxicity Prediction (ProTox-II)

Comparative toxicity predictions are shown in Table 3.

Table 3: ProTox-II toxicity predictions.

Parameter	Chitranone	Droserone	Doxorubicin
Predicted LD_{50} (mg/kg)	1000	707	205
Toxicity Class	4	4	3
Hepatotoxicity	Inactive (0.63)	Inactive (0.6)	Inactive (0.86)
Neurotoxicity	Inactive (0.78)	Inactive (0.84)	Active (0.74)
Nephrotoxicity	Active (0.56)	Active (0.50)	Active (0.80)
Respiratory Toxicity	Active (0.66)	Active (0.66)	Active (0.91)
Cardiotoxicity	Inactive (0.84)	Inactive (0.78)	Active (0.64)
Immunotoxicity	Active (0.95)	Active (0.52)	Active (0.99)
Mutagenicity	Inactive (0.74)	Active (0.73)	Active (0.98)
Cytotoxicity	Inactive (0.68)	Inactive (0.71)	Active (0.94)
BBB Barrier	Active (0.51)	Active (0.50)	Inactive (1.0)
Clinical Toxicity	Active (0.58)	Active (0.63)	Active (0.84)

4. DISCUSSION

The present in silico investigation reveals that chitranone demonstrates remarkable binding affinity (−10.5 kcal/mol) to the EGFR kinase domain, surpassing doxorubicin by 1.7 kcal/mol. This difference is pharmacologically significant, as each kcal/mol corresponds to approximately a 5-fold change in binding constant at physiological temperature.[22] Both chitranone (−10.5 kcal/mol) and droserone (−7.1 kcal/mol) exceeded the −7.0 kcal/mol threshold indicating strong binding.[23]

Chitranone's superior affinity derives from its expanded bi-naphthoquinone scaffold enabling 16 interactions including nine pi-alkyl contacts, complemented by hydrogen bonds with catalytically important ARG858 and ASP855 residues. The L858R mutation in 8A2B is one of the most common activating mutations in EGFR-driven NSCLC. Chitranone's favorable interaction with this mutant suggests relevance for targeting clinically important EGFR variants.

The interaction profiles overlap substantially between chitranone and droserone at key residues LEU788, MET766, LEU777, ASP855, and ARG858, which span the hinge region and activation loop critical for kinase catalytic activity.[24,25] PHE723 engagement via pi-pi T-shaped interaction mirrors patterns observed for established EGFR inhibitors gefitinib and erlotinib.[24] Droserone's recently reported anti-austerity activity against PANC-1 cells via Akt pathway suppression, combined with its EGFR binding demonstrated here, suggests multi-target therapeutic potential along the EGFR–Akt axis.[26]

The ADMET analysis reveals markedly superior drug-likeness for both naphthoquinones compared to doxorubicin. Zero Lipinski violations, high gastrointestinal absorption, and absence of P-gp substrate activity contrast sharply with doxorubicin's three Lipinski violations and P-gp substrate status that contributes to multidrug resistance.[27,28] Droserone's bioavailability score (0.85) was highest among all compounds. The absence of cardiotoxicity predictions for both naphthoquinones contrasts favorably with doxorubicin's well-documented dose-limiting cardiotoxicity.[29] Higher LD_{50} values (chitranone: 1000 mg/kg; droserone: 707 mg/kg) compared to doxorubicin (205 mg/kg) further support improved safety profiles.

PAINS alerts for quinone-containing structural motifs[30] necessitate careful experimental validation to distinguish genuine target-specific activity from assay artifacts. The predicted mutagenicity of droserone requires investigation via appropriate genotoxicity assays. Synthetic accessibility scores indicate droserone (2.62) is more readily synthesizable than chitranone (3.52), potentially influencing development feasibility. These findings align with recent network pharmacology studies identifying EGFR as a key P. zeylanica target in breast and prostate cancers[26,31], extending knowledge to specific chitranone and droserone interactions.

It should be noted that molecular docking represents a preliminary computational assessment. Predicted affinities require validation through enzyme inhibition kinetics, cell-based proliferation assays, and ultimately in vivo efficacy studies. The anti-cell proliferation effects of other P. zeylanica naphthoquinone dimers, such as maritinone, have been experimentally confirmed[32], providing precedent for the potential bioactivity of structurally related chitranone.

5. CONCLUSION

This study demonstrates that chitranone from P. zeylanica exhibits superior binding affinity (−10.5 kcal/mol, 16 interactions) to the EGFR kinase domain compared to doxorubicin (−8.8 kcal/mol, 11 interactions), with extensive hydrogen bond, electrostatic, and hydrophobic interactions at key active site residues. Droserone also showed favorable binding (−7.1 kcal/mol) with excellent drug-likeness (bioavailability score: 0.85). Both naphthoquinones demonstrated superior ADMET profiles with zero Lipinski violations, high GI absorption, no P-gp substrate activity, and lower predicted toxicity than doxorubicin. These findings provide a strong rationale for experimental validation of chitranone and droserone as potential anti-EGFR anticancer agents.

CONFLICTS OF INTEREST

The author declares no conflicts of interest.

ACKNOWLEDGMENTS

The author acknowledges the use of publicly available databases including RCSB PDB, PubChem, IMPPAT, SwissADME, and ProTox-II.

REFERENCES

1. Sung H, Ferlay J, Siegel RL, Laversanne M, Soerjomataram I, Jemal A, et al. Global Cancer Statistics 2020: GLOBOCAN Estimates of Incidence and Mortality Worldwide for 36 Cancers in 185 Countries. CA Cancer J Clin., 2021; 71(3): 209–49. doi:10.3322/caac.21660 PubMed PMID: 33538338.
2. Yarden Y, Sliwkowski MX. Untangling the ErbB signalling network. Nat Rev Mol Cell Biol., 2001; 2(2): 127–37. doi:10.1038/35052073
3. Ferguson KM. Structure-based view of epidermal growth factor receptor regulation. Annu Rev Biophys, 2008; 37: 353–73. doi:10.1146/annurev.biophys.37.032807.125829 PubMed PMID: 18573086; PubMed Central PMCID: PMC2745238.
4. Newman DJ, Cragg GM. Natural Products as Sources of New Drugs over the Nearly Four Decades from 01/1981 to 09/2019. J Nat Prod., 2020; 83(3): 770–803. doi:10.1021/acs.jnatprod.9b01285
5. Roy A, Bharadvaja N. A review on pharmaceutically important medical plant: Plumbago zeylanica. Journal of Ayurvedic and Herbal Medicine, 2017; 3(4): 225–8.
6. Sundari BKR, Telapolu S, Dwarakanath BS, Thyagarajan SadrasP. Cytotoxic and Antioxidant Effects in Various Tissue Extracts of Plumbago zeylanica: Implications for Anticancer Potential. PJ., 2017; 9(5): 706–12. doi:10.5530/pj.2017.5.111
7. Aziz MH, Dreckschmidt NE, Verma AK. Plumbagin, a Medicinal Plant–Derived Naphthoquinone, Is a Novel Inhibitor of the Growth and Invasion of Hormone-Refractory Prostate Cancer. Cancer Research. 2008; 68(21): 9024–32. doi:10.1158/0008-5472.CAN-08-2494
8. Lin LC, Yang LL, Chou CJ. Cytotoxic naphthoquinones and plumbagic acid glucosides from Plumbago zeylanica. Phytochemistry, 2003; 62(4): 619–22. doi:10.1016/s0031-9422(02)00519-8 PubMed PMID: 12560036.
9. Jamal MS, Parveen S, Beg MA, Suhail M, Chaudhary AGA, Damanhouri GA, et al. Anticancer compound plumbagin and its molecular targets: a structural insight into the inhibitory mechanisms using computational approaches. PLoS One, 2014; 9(2): e87309. doi:10.1371/journal.pone.0087309 PubMed PMID: 24586269; PubMed Central PMCID: PMC3937309.
10. Cao YY, Yu J, Liu TT, Yang KX, Yang LY, Chen Q, et al. Plumbagin inhibits the proliferation and survival of esophageal cancer cells by blocking STAT3-PLK1-AKT signaling. Cell Death Dis., 2018; 9(2): 17. doi:10.1038/s41419-017-0068-6

PubMed PMID: 29339720; PubMed Central PMCID: PMC5833725.
11. Yin Z, Zhang J, Chen L, Guo Q, Yang B, Zhang W, et al. Anticancer Effects and Mechanisms of Action of Plumbagin: Review of Research Advances. Biomed Res Int., 2020; 2020: 6940953. doi:10.1155/2020/6940953 PubMed PMID: 33344645; PubMed Central PMCID: PMC7725562.
12. Roy A. Plumbagin: A Potential Anti-cancer Compound. Mini Rev Med Chem., 2021; 21(6): 731–7. doi:10.2174/1389557520666201116144421 PubMed PMID: 33200707.
13. Gunaherath GMKB, Gunatilaka AAL, Thomson RH. Studies on medicinal and related plants of Sri Lanka. Part 18. Structure of a new naphthoquinone from Plumbago zeylanica. Journal of The Chemical Society-perkin Transactions 1 [Internet], 1988; 407–10. Available from: https://api.semanticscholar.org/CorpusID:97924101
14. Raj G, Kurup R, Hussain AA, Baby S. Distribution of naphthoquinones, plumbagin, droserone, and 5-O-methyl droserone in chitin-induced and uninduced Nepenthes khasiana: molecular events in prey capture. J Exp Bot., 2011; 62(15): 5429–36. doi:10.1093/jxb/err219 PubMed PMID: 21862483.
15. Meng XY, Zhang HX, Mezei M, Cui M. Molecular docking: a powerful approach for structure-based drug discovery. Curr Comput Aided Drug Des., 2011; 7(2): 146–57. doi:10.2174/157340911795677602 PubMed PMID: 21534921; PubMed Central PMCID: PMC3151162.
16. Maneenet J, Tajuddeen N, Hong Nguyen H, Fujii R, Kimbadi Lombe B, Feineis D, et al. Droserone and dioncoquinone B, and related naphthoquinones as potent antiausterity agents against human PANC-1 pancreatic cancer cells. Results in Chemistry, 2024; 7: 101352. doi:10.1016/j.rechem.2024.101352
17. Mohanraj K, Karthikeyan BS, Vivek-Ananth RP, Chand RPB, Aparna SR, Mangalapandi P, et al. IMPPAT: A curated database of Indian Medicinal Plants, Phytochemistry And Therapeutics. Sci Rep., 2018; 8(1): 4329. doi:10.1038/s41598-018-22631-z PubMed PMID: 29531263; PubMed Central PMCID: PMC5847565.
18. Laskowski RA, MacArthur MW, Moss DS, Thornton JM. ıt PROCHECK: a program to check the stereochemical quality of protein structures. Journal of Applied Crystallography, 1993; 26(2): 283–91. doi:10.1107/S0021889892009944
19. Trott O, Olson AJ. AutoDock Vina: improving the speed and accuracy of docking with a new scoring function, efficient optimization, and multithreading. J Comput Chem., 2010; 31(2): 455–61. doi:10.1002/jcc.21334 PubMed PMID: 19499576; PubMed Central PMCID: PMC3041641.
20. Daina A, Michielin O, Zoete V. SwissADME: a free web tool to evaluate pharmacokinetics, drug-likeness and medicinal chemistry friendliness of small molecules. Sci Rep., 2017; 7: 42717. doi:10.1038/srep42717 PubMed PMID: 28256516; PubMed Central PMCID: PMC5335600.
21. Banerjee P, Eckert AO, Schrey AK, Preissner R. ProTox-II: a webserver for the prediction of toxicity of chemicals. Nucleic Acids Res., 2018; 46(W1): W257–63. doi:10.1093/nar/gky318 PubMed PMID: 29718510; PubMed Central PMCID: PMC6031011.
22. Kuntz ID, Blaney JM, Oatley SJ, Langridge R, Ferrin TE. A geometric approach to macromolecule-ligand interactions. J Mol Biol., 1982; 161(2): 269–88. doi:10.1016/0022-2836(82)90153-x PubMed PMID: 7154081.
23. Nandi A, Nigar T, Das A, Dey YN. Network pharmacology analysis of *Plumbago zeylanica* to identify the therapeutic targets and molecular mechanisms involved in ameliorating hemorrhoids. Journal of Biomolecular Structure and Dynamics, 2023; 1–15. doi:10.1080/07391102.2023.2280681
24. Stamos J, Sliwkowski MX, Eigenbrot C. Structure of the epidermal growth factor receptor kinase domain alone and in complex with a 4-anilinoquinazoline inhibitor. J Biol Chem., 2002; 277(48): 46265–72. doi:10.1074/jbc.M207135200 PubMed PMID: 12196540.
25. Yun CH, Boggon TJ, Li Y, Woo MS, Greulich H, Meyerson M, et al. Structures of lung cancer-derived EGFR mutants and inhibitor complexes: mechanism of activation and insights into differential inhibitor sensitivity. Cancer Cell, 2007; 11(3): 217–27. doi:10.1016/j.ccr.2006.12.017 PubMed PMID: 17349580; PubMed Central PMCID: PMC1939942.
26. Siddiqui AJ, Alshammari AM, Patel M, Ghoniem AEM, Siddiqui MA, Abdalla RAH, et al. Anti-cancer effects of Plumbago zeylanica L. against human triple-negative breast cancer: Insights from network pharmacology and in-vitro experimental validation. South African Journal of Botany [Internet], 2025. Available from: https://api.semanticscholar.org/CorpusID:277658897
27. Lipinski CA, Lombardo F, Dominy BW, Feeney PJ. Experimental and computational approaches to estimate solubility and permeability in drug discovery and development settings. Adv Drug Deliv Rev., 2001; 46(1–3): 3–26. doi:10.1016/s0169-409x(00)00129-0 PubMed PMID: 11259830.
28. Aller SG, Yu J, Ward A, Weng Y, Chittaboina S, Zhuo R, et al. Structure of P-glycoprotein reveals a molecular basis for poly-specific drug binding. Science, 2009; 323(5922): 1718–22. doi:10.1126/science.1168750 PubMed PMID: 19325113; PubMed Central PMCID: PMC2720052.
29. Carvalho C, Santos RX, Cardoso S, Correia S, Oliveira PJ, Santos MS, et al. Doxorubicin: the good, the bad and the ugly effect. Curr Med Chem., 2009; 16(25): 3267–85. doi:10.2174/092986709788803312 PubMed PMID: 19548866.

30. Baell JB, Holloway GA. New substructure filters for removal of pan assay interference compounds (PAINS) from screening libraries and for their exclusion in bioassays. J Med Chem., 2010; 53(7): 2719–40. doi:10.1021/jm901137j PubMed PMID: 20131845.
31. Zrinej J, Ouabane M, Mchichi LE, Qara A, Sekkate C, Lakhlıfı T, et al. Chemical and biological evaluation of the Plumbago Zeylanica plant against prostate cancer. A unified approach combining molecular docking, dynamic simulations, pharmacophore modeling, DFT and ADMET studies. Vietnam Journal of Chemistry [Internet], 2025. Available from: https://api.semanticscholar.org/CorpusID:276982183
32. Ito C, Matsui T, Takano M, Wu TS, Itoigawa M. Anti-cell proliferation effect of naphthoquinone dimers isolated from Plumbago zeylanica. Nat Prod Res., 2018; 32(18): 2127–32. doi:10.1080/14786419.2017.1366476 PubMed PMID: 28823173.